

## ACOUSTIC RESONATORS – A METHOD FOR ONLINE STUDY IN DETERMINING THE SPEED OF SOUND IN AIR

FABIOLA SANDA CHIRIACESCU<sup>1,2</sup>, B. CHIRIACESCU<sup>1,2</sup>, CRISTINA MIRON<sup>1,\*</sup>,  
C. BERLIC<sup>1,\*</sup>, V. BARNA<sup>1</sup>

<sup>1</sup>University of Bucharest, Faculty of Physics, 405 Atomistilor Street, 077125, Magurele, Romania

<sup>2</sup>“Nicolae Iorga”, Theoretical High School 1 Scolii Street, 125100, Nehoiu, Romania

\*Corresponding authors: *cmiron\_2001@yahoo.com, cberlic@gmail.com*

*Received December 16, 2020*

*Abstract.* In this paper, we present an alternative experiment for measuring the speed of sound in air by finding the frequency and the wavelength of the stationary sound waves formed in a closed-end tube. The experiment involved both video and sound recording, the files were afterward analyzed by using two free and open-source computer software, namely Audacity and Kdenlive. The research described herein is intended for the students interested in emphasizing the learning of physics by inquiry-based experiment, yet represents a viable alternative for developing long-distance studies.

*Key words:* acoustic resonators, speed of sound, video and audio analysis, online study, inquiry based experiment.

### 1. INTRODUCTION

The study and understanding of sound is an important topic in physics, because acoustic waves exist everywhere and are acting in our daily activities and life [1]. Experiments of acoustics for university level students are classical and widely studied in physics classes.

In addition, the resonance phenomena are studied by means of a vertical tube partially filled with water and a dedicated speaker. The sound can be detected/recorded by a microphone or directly heard by the human ear in the laboratory [2, 3], the tube becoming an acoustic resonator [4]. The operation of acoustic resonators is based on the resonance phenomenon that occurs in standing waves. Pipes provide an interesting platform for students to understand how variations in the tube length modify the amplitude of the standing waves and therefore greatly help them to better comprehend the physics behind the present experiment [5].

The paper aims an experimental exploration illustrating a novel approach of general interest, while using inexpensive and simple equipment. The research illustrated herein is intended for the students interested in emphasizing the learning of physics by inquiry-based experiment.

Several works present these approaches to various subjects of physics learning using well-suited software. An indication of several recent studies that describe reasonably priced and uncomplicated video analysis experiments and software tools in classical mechanics addressed to university and high school levels can be found here [6–9].

In this paper, our main purpose is measuring the speed of sound by finding the frequency and the wavelength of the sound waves that are contained in a particular tube system having a closed-end. For this work, a closed pipe of variable length is employed. The length of the tube is varied by filling it with water and finding the positions of nodes and antinodes for several frequencies of the sound emitted by a speaker inside the system.

To achieve greater precision for our measurements, two free and open-source computer software are used – Audacity and Kdenlive. Audacity [10] is specially employed for audio analysis and sound editing. It can be installed on any Operating System (Windows, Mac or Linux) and it is a very versatile and easy to use (intuitive) program. The Audacity software is used to record, edit and analyze sound waves [11–15]. It can be also generally employed as an education tool in physics classes, including experiments where students play musical instruments and study the resulting sounds in terms of time and frequency [16–18].

Kdenlive [19] is an important open-source software tool for video editing. The initial code was developed for Linux, but now it can be installed also under Windows and MacOS. We chose this software for the video analysis of the experiment because the program is straightforward, yet precise, offering similar performances to any established professional software.

The proposed physics laboratory research for the present article is clearly a viable alternative for developing long-distance studies (especially when considering the difficult current times).

## 2. EXPERIMENTAL SETUP

The experimental setup consists in a cylindrical tube made of glass (1.4 m length, Fig. 1). At the lower end, the tube is connected with a water supply inlet, which gives the possibility to fill or to empty the tube with water. This way, the length of the air column inside the tube can be varied at the user's choice. Using a faucet, the filling and the emptying speed can also be accurately controlled. The portion of the tube between the free surface of the water and the upper end of the tube actually corresponds to the acoustic resonator.

At the upper end of the tube, we have a loudspeaker connected to a frequency generator, representing the audio source that produces the sounds with known characteristics. After traveling through the tube, the waves are then back-reflected

by the water surface and, due to the interference between the direct wave and the reflected one, nodes and antinodes are formed [20, 21]. The nodes and antinodes are the results of the resonance phenomenon that occurs in standing waves, the tube being in fact an acoustic resonator.

The distance between two successive nodes or antinodes (where we have a maximum or respectively a minimum intensity of the sound) is  $\lambda/2$ , where  $\lambda$  is the wavelength of the sound [4, 22–24]. If we manage to measure these distances, we can subsequently calculate the wavelength and find the speed of the sound from the following relation

$$c = \lambda \cdot \nu \quad (1)$$

where  $\nu$  is the frequency of the propagating sound.

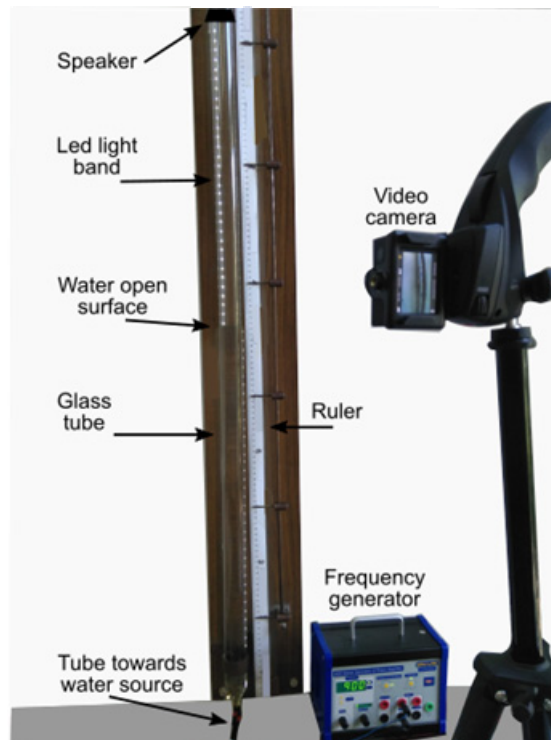


Fig. 1 – Experimental setup for our experiment. The full color version may be accessed at <http://www.rrp.nipne.ro>.

In order to find the precise positions of the nodes and antinodes that form inside the resonator, a ruler having the long axis parallel with the tube is installed. For better observation of the surface of the water, a luminescent LED (Light

Emitting Diode) band was attached parallel with the tube axis. Due to the refraction phenomenon, the images of the LEDs change their position, “crossing” from one side of the tube to the other, as it can be perceived in Fig. 2, offering a qualitative indication of the position where the free surface of the water is at a certain moment in time.

The position of the water surface is recorded with an action type video camera (Senso AT-30S Sport 4K with 4k pixel resolution, 30 fps shutter speed). Simultaneously, the sound produced in the resonator is recorded as a soundtrack. When later analyzing the recordings, we can find the accurate position where the sound has a maximum or minimum intensity, corresponding to nodes, respectively antinodes in the propagating waveform.



Fig. 2 – Image of the free surface of the water and the “crossing” of the LEDs light images due to the refraction phenomenon. The full color version may be accessed at <http://www.rrp.nipne.ro>.

### 3. RESULTS AND DISCUSSIONS

Using the frequency generator settings, we choose a sound amplitude that is loud enough to ensure a good quality of the recorded soundtrack. The video camera parameters are also tuned for having the best quality of the image.

The filling and the emptying processes of the tube have been recorded both video and audio for sound waves frequencies values starting from 500 Hz and going up to 1400 Hz.

For improved movie quality, environmental noise such as human speaking and other accidental/ambient sounds were avoided. Afterward, during the post-processing phase, the Audacity software allows “cleaning” the background sound that cannot be avoided (for example, the sound made by the flowing water through the tube, or in the sewerage). In order to have a reference background sound, we record the filling and the emptying processes, without the frequency generator started.

Each sample was firstly uploaded in the Audacity software. As we mentioned before, the software is especially used for editing and analyzing audio files. Subsequently, the background noises identified during the recording are cleaned. Audacity can provide visualization of the wave aspect depending on the noise amplitude, Fig. 3, or the frequencies spectra of the recorded sounds, Fig. 4.

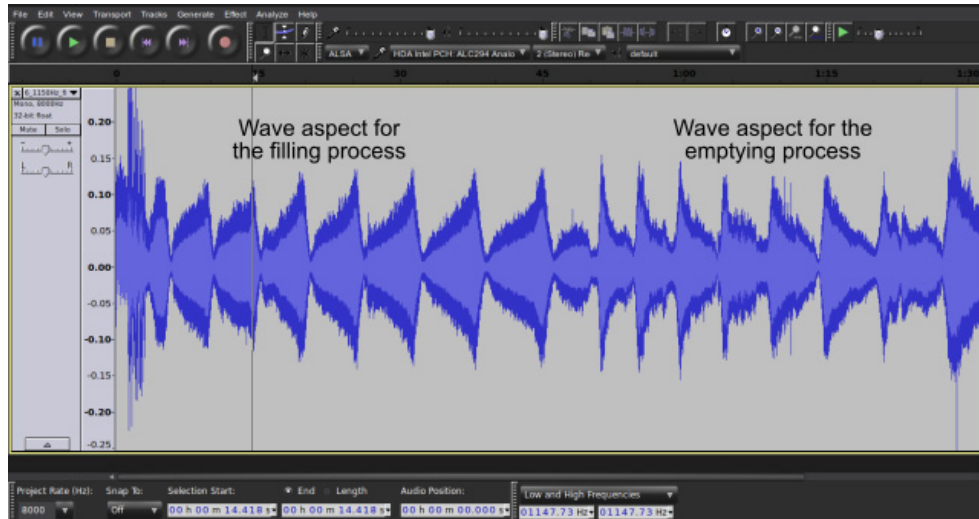


Fig. 3 – Wave aspect according to the amplitude, as obtained with Audacity software. The full color version may be accessed at <http://www.rrp.nipne.ro>.

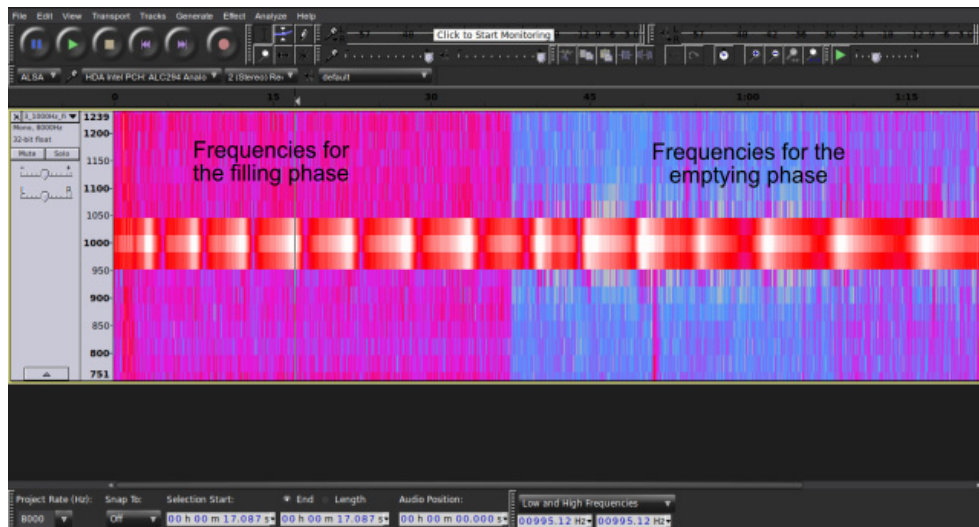


Fig. 4 – Frequencies spectrum, as obtained with Audacity software. The full color version may be accessed at <http://www.rrp.nipne.ro>.

One can notice from Fig. 4 that the frequency spectrum is quite different in the filling phase of the tube with respect to the emptying stage. In the filling phase, the red color prevails, indicating a more pronounced background noise. This is due to the noise from the water source, noise that is consequently missing when considering the emptying stage. Meanwhile, interference maximums and minimums can be observed – maximums are indicated by a brighter color and minimums are areas where the waves are interrupted.

Using one of the diagrams (either amplitude or frequency spectrum), we find the time instants corresponding to maximum or minimum (nodes and antinodes), both for the filling and for the emptying phase. The program allows for detecting these time moments with high precision (millisecond range).

An alternative software used for collecting and analyzing data is Kdenlive. This also offers the possibility to visualize the audio wave spectra. Once we found the time moments corresponding to the nodes or antinodes, Kdenlive software was used to find positions where the nodes or antinodes are situated. The software works with a frequency of 25 frames per second (fps), leading to a very good precision in finding the moments of maximum or minimum of sound wave interference.

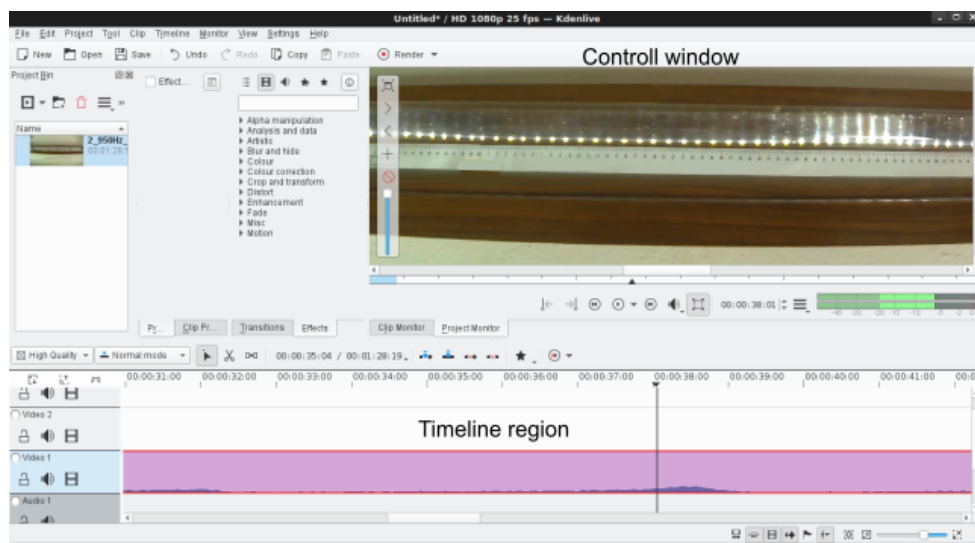


Fig. 5 – Main screen of the Kdenlive software. The full color version may be accessed at <http://www.rrp.nipne.ro>.

Using the previously obtained time instants, we can accurately establish the positions of the free surface of the water corresponding to a node or an antinode on the ruler markings. As we discussed earlier, the distance between two consecutive nodes or two antinodes is the measure for half of the wavelength of the propagating sound.

The obtained experimental values are presented in Tables 1–4.

Table 1

Results obtained analyzing the antinodes positions during the tube's filling stage

| v (Hz) | $\lambda_1$ (m) | $\lambda_2$ (m) | $\lambda_3$ (m) | $\lambda_4$ (m) | $\lambda_5$ (m) | $\bar{\lambda}$ (m) | $c = \lambda \cdot v$<br>(m/s) | $\bar{c}$<br>(m/s) |
|--------|-----------------|-----------------|-----------------|-----------------|-----------------|---------------------|--------------------------------|--------------------|
| 900    | 0.382           | 0.380           | 0.391           | 0.379           | 0.381           | 0.383               | 344                            | 343.5 ± 0.0480     |
| 950    | 0.352           | 0.358           | 0.373           | 0.357           | 0.370           | 0.362               | 344                            |                    |
| 1000   | 0.346           | 0.340           | 0.344           | 0.348           | 0.342           | 0.344               | 344                            |                    |
| 1050   | 0.327           | 0.328           | 0.330           | 0.325           | 0.324           | 0.327               | 343                            |                    |
| 1100   | 0.315           | 0.307           | 0.314           | 0.330           | 0.296           | 0.312               | 344                            |                    |
| 1150   | 0.297           | 0.303           | 0.281           | 0.303           | 0.307           | 0.298               | 343                            |                    |
| 1200   | 0.274           | 0.301           | 0.291           | 0.279           | 0.286           | 0.286               | 343                            |                    |
| 1250   | 0.269           | 0.281           | 0.258           | 0.282           | 0.284           | 0.275               | 344                            |                    |
| 1300   | 0.277           | 0.265           | 0.262           | 0.258           | 0.260           | 0.264               | 344                            |                    |
| 1350   | 0.256           | 0.262           | 0.253           | 0.251           | 0.249           | 0.254               | 343                            |                    |
| 1400   | 0.245           | 0.244           | 0.253           | 0.239           | 0.247           | 0.246               | 343                            |                    |

Table 2

Results obtained analyzing the antinodes positions during the tube's emptying stage

| v (Hz) | $\lambda_1$ (m) | $\lambda_2$ (m) | $\lambda_3$ (m) | $\lambda_4$ (m) | $\lambda_5$ (m) | $\bar{\lambda}$ (m) | $c = \lambda \cdot v$<br>(m/s) | $\bar{c}$ (m/s) |
|--------|-----------------|-----------------|-----------------|-----------------|-----------------|---------------------|--------------------------------|-----------------|
| 900    | 0.373           | 0.359           | 0.402           | 0.401           | 0.373           | 0.382               | 343                            | 343.4 ± 0.0698  |
| 950    | 0.359           | 0.360           | 0.353           | 0.373           | 0.361           | 0.361               | 343                            |                 |
| 1000   | 0.357           | 0.339           | 0.338           | 0.350           | 0.335           | 0.344               | 344                            |                 |
| 1050   | 0.328           | 0.332           | 0.327           | 0.319           | 0.328           | 0.327               | 343                            |                 |
| 1100   | 0.301           | 0.320           | 0.303           | 0.327           | 0.311           | 0.312               | 344                            |                 |
| 1150   | 0.308           | 0.294           | 0.294           | 0.301           | 0.296           | 0.299               | 343                            |                 |
| 1200   | 0.316           | 0.287           | 0.259           | 0.293           | 0.274           | 0.286               | 343                            |                 |
| 1250   | 0.270           | 0.271           | 0.302           | 0.262           | 0.270           | 0.275               | 344                            |                 |
| 1300   | 0.265           | 0.262           | 0.262           | 0.265           | 0.268           | 0.264               | 344                            |                 |
| 1350   | 0.254           | 0.252           | 0.258           | 0.252           | 0.256           | 0.254               | 343                            |                 |
| 1400   | 0.246           | 0.254           | 0.248           | 0.247           | 0.232           | 0.245               | 343                            |                 |

The values of the speed of sound obtained from positions of nodes and antinodes in both filling and emptying of the tubes are very close one to another, indicating the consistency of our experimental approaches and method in general. The average obtained value is 343.5 m/s, a result that corresponds to a 20.4°C temperature listed from the literature [21, 25]. The measured temperature in the lab during the experiments was 21.0°C; again, this result is in very good agreement with the above mentioned theoretical value.

The acquired results are particularly satisfactory, taking into consideration as well the eventual error sources. The first error source is the loss in the quality of

the recordings due to the incomplete elimination of the background noise. We have to remark here that, in the filling and in the emptying processes, the noise of the running water was removed by using the “Noise reduction” processing feature in the Audacity program.

Table 3

Results obtained analyzing the nodes' positions during the tube's filling stage

| v (Hz) | $\lambda_1$ (m) | $\lambda_2$ (m) | $\lambda_3$ (m) | $\lambda_4$ (m) | $\bar{\lambda}$ (m) | $c = \lambda \cdot v$<br>(m/s) | $\bar{c}$ (m/s) |
|--------|-----------------|-----------------|-----------------|-----------------|---------------------|--------------------------------|-----------------|
| 900    | 0.384           | 0.387           | 0.384           | 0.372           | 0.382               | 344                            | 343.7 ± 0.0598  |
| 950    | 0.361           | 0.362           | 0.359           | 0.365           | 0.362               | 344                            |                 |
| 1000   | 0.343           | 0.348           | 0.339           | 0.344           | 0.344               | 344                            |                 |
| 1050   | 0.324           | 0.327           | 0.329           | 0.328           | 0.327               | 343                            |                 |
| 1100   | 0.311           | 0.308           | 0.314           | 0.317           | 0.313               | 344                            |                 |
| 1150   | 0.300           | 0.301           | 0.297           | 0.298           | 0.299               | 344                            |                 |
| 1200   | 0.286           | 0.286           | 0.287           | 0.285           | 0.286               | 343                            |                 |
| 1250   | 0.276           | 0.275           | 0.276           | 0.273           | 0.275               | 344                            |                 |
| 1300   | 0.267           | 0.263           | 0.268           | 0.260           | 0.265               | 344                            |                 |
| 1350   | 0.255           | 0.254           | 0.254           | 0.254           | 0.254               | 343                            |                 |
| 1400   | 0.252           | 0.241           | 0.248           | 0.241           | 0.246               | 344                            |                 |

Table 4

Results obtained analyzing the nodes' positions during the tube's emptying stage

| v (Hz) | $\lambda_1$ (m) | $\lambda_2$ (m) | $\lambda_3$ (m) | $\lambda_4$ (m) | $\bar{\lambda}$ (m) | $c = \lambda \cdot v$<br>(m/s) | $\bar{c}$ (m/s) |
|--------|-----------------|-----------------|-----------------|-----------------|---------------------|--------------------------------|-----------------|
| 900    | 0.382           | 0.380           | 0.385           | 0.379           | 0.382               | 343                            | 343.5 ± 0.0748  |
| 950    | 0.359           | 0.361           | 0.364           | 0.362           | 0.362               | 343                            |                 |
| 1000   | 0.341           | 0.339           | 0.347           | 0.346           | 0.343               | 343                            |                 |
| 1050   | 0.328           | 0.327           | 0.327           | 0.328           | 0.328               | 344                            |                 |
| 1100   | 0.313           | 0.311           | 0.312           | 0.313           | 0.312               | 343                            |                 |
| 1150   | 0.298           | 0.296           | 0.301           | 0.300           | 0.299               | 344                            |                 |
| 1200   | 0.288           | 0.282           | 0.287           | 0.288           | 0.286               | 344                            |                 |
| 1250   | 0.278           | 0.272           | 0.270           | 0.279           | 0.275               | 343                            |                 |
| 1300   | 0.264           | 0.266           | 0.263           | 0.264           | 0.264               | 344                            |                 |
| 1350   | 0.257           | 0.254           | 0.256           | 0.251           | 0.255               | 344                            |                 |
| 1400   | 0.248           | 0.243           | 0.243           | 0.248           | 0.246               | 344                            |                 |

Another error source was present due to the image resolution, which can occasionally lead to minor variations when reading the values on the vertical ruler.

The last error source we had to overcome was concerning the video camera being fixed in the middle region of the tube. This situation can lead to errors in



reading the positions of the free water surface in the key moments – represented by the maximum or minimum of interference. When the free surface of the water is situated in the median part of the tube, the reading is more precise, as we look perpendicularly at the tube, including here the water column and the attached ruler. Towards the ends of the tube (superior and inferior alike), the reading is accomplished under a certain angle and this leads to reading errors, as illustrated in Fig. 6.

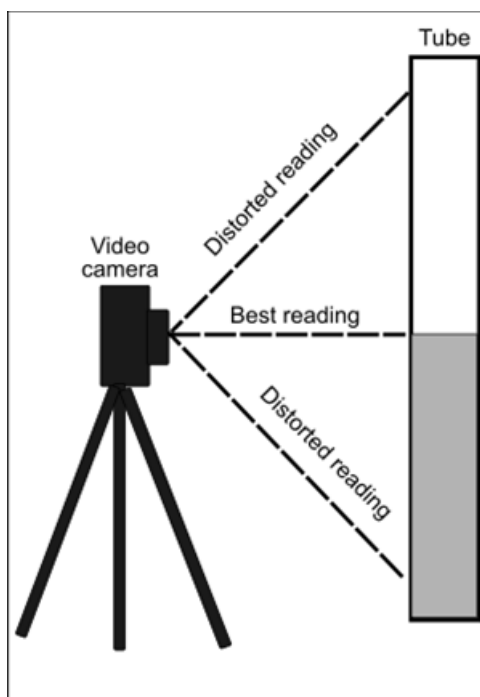


Fig. 6 – Errors in the reading process due to the angle under which the experimental recording is performed. The full color version may be accessed at <http://www.rpp.nipne.ro>.

Despite all these error sources, the obtained results are virtually similar to the theoretical value of the speed of sound in air, which clearly validates the experimental method we proposed for this study.

#### 4. CONCLUSIONS

In this paper, we describe an experimental approach for the measurement of the speed of sound in the air environment. The experimental setup employed in conjunction with video and audio analysis software turned out to be a highly reliable tool, suitable for obtaining very good investigational results for high school physics classes.

The entire study described herein can be exploited (and even further expanded) by students, because it is relatively straightforward to collect the data and perform the afterward analysis. We also remark the didactical advantage of the approach as it is conceptually very simple, consisting of finding the positions of minima and maxima for the sound intensity in the tube, by using the right software support.

The described method is a great alternative for organizing a long-distance (online) experiment: the students receive the audio and video recordings (*via* e-mail for example) and subsequently they can individually make measurements and calculate the associated physical quantities in conditions of distance learning.

#### REFERENCES

1. M. K. Kasar, K. Yurumezoglu and S. K. Sengoren, *Phys. Teach.* **50**, 558–559 (2012).
2. R. J. Fajardo, *Phys. Teach.* **16**, 313–316 (1978).
3. N. L. Barreiro, A. S. Vallespi, N. M. Zajarevich, A. L. Peuriot and V. B. Slezak, *Eur. J. Phys.* **38**(5), 055805 (2017).
4. E. S. Barna, C. Ciucu, V. Barna, C. Miron and C. Berlic, *Lucrări practice. Mecanică fizică și acustică*, Edit. Universității București, Bucharest, 2010.
5. S. Bhagwat and M. A. Creasy, *Eur. J. Phys.* **38**(3), 035003 (2017).
6. B. Chiriacescu, F. S. Chiriacescu, C. Miron, C. Berlic and V. Barna, *Rom. Rep. Phys.* **72**, 901 (2020).
7. S. Trocaru, C. Berlic, C. Miron and V. Barna, *Rom. Rep. Phys.* **72**, 902 (2020).
8. F. S. Chiriacescu, B. Chiriacescu, C. Miron, C. Berlic and V. Barna, *Rom. Rep. Phys.* **72**, 904 (2020).
9. B. Chiriacescu, F. S. Chiriacescu and S. Voinea, *Rom. Rep. Phys.* **73**, 901 (2021).
10. <https://www.audacityteam.org/>
11. D. E. Asbanu and U. Babys, *Int. J. Sci. Res.* **6**(11), 324–329 (2017).
12. M. A. Dias, P. S. Carvalho and D. R. Ventura, *Phys. Educ.* **51**, 035–002 (2016).
13. R. Jaafar and A. N. Daud, *Harmonic series experiments in three-in-one resonance tube with Audacity software*, IOP Conference Series: Journal of Physics: Conference Series **1185**, 012132 (2019).
14. Y. Pramudya, L. Widayanti and F. Melliagrina, *Frequency Measurement of Bonang-Barung and Peking in Javanese Gamelan using Audacity*, IOP Conference Series: Journal of Physics: Conference Series **1075**, 012047 (2018).
15. J. A. Gomez-Tejedor, J. C. Castro-Palacio and J. A. Monsoriu, *Phys. Educ.* **49**(3), 310–313 (2014).
16. B. Brazzle, *Phys. Teach.* **49**(4), 228–230 (2011).
17. A. C. Courtney and M. W. Courtney, *Phys. Educ.* (2012) arXiv ID: 1211.4832.
18. M. C. LoPresto, *Phys. Educ.* **43**, 30–36 (2008).
19. <https://kdenlive.org/en/>
20. D. Halliday, R. Resnick, J. Walker, *Fundamentals of Physics Extended*, 9<sup>th</sup> Edition, Wiley, 2010.
21. S. Velasco, F. L. Román, A. González and J. A. White, *Am. J. Phys.* **72**(2), 276–279 (2004).
22. A. Hristev, *Mecanică și acustică*, Edit. Didactică și Pedagogică, Bucharest, 1984.
23. A. P. French, *Vibrations and Waves*, The M.I.T. Introductory Physics Series, CBS Publishers & Distributors, 2003.
24. R. Fitzpatrick, *Oscillations and Waves: An Introduction*, 1<sup>st</sup> Edition, CRC Press, 2017.
25. P. J. Ouseph and J. J. Link, *Am. J. Phys.* **52**(7), 661 (1984).